

Communication

1.55 μm Narrow-Linewidth Pulsed Laser Based on MgO:PPLN

Yaling Yang¹, Guorui Lv^{2,3}, Lei Guo^{1,2,*}, Haiping Xu^{2,3}, Hui Kong^{2,3}, Jiaqi Wen^{2,3}, Jintian Bian^{2,3,*}, Qing Ye^{2,3} , Kejian Yang⁴ and Jingliang He⁴

¹ School of Mechanics and Optoelectronic Physics, Anhui University of Science and Technology, Huainan 232001, China

² State Key Laboratory of Pulsed Power Laser Technology, National University of Defense Technology, Hefei 230037, China

³ Advanced Laser Technology Laboratory of Anhui Province, Hefei 230037, China

⁴ State Key Laboratory of Crystal Materials, Institute of Novel Semiconductors, Shandong University, Jinan 250100, China

* Correspondence: leiguo@aust.edu.cn (L.G.); bianjintian17@nudt.edu.cn (J.B.)

Abstract: A high-power narrow-linewidth 1.55 μm pulsed laser, based on MgO:PPLN OPO, has been achieved using a F–P etalon. The pump source is a 1064 nm acousto-optical (AO) Q-switched Nd:YAG laser with a repetition rate of 10 kHz. Under the maximum pump power of 18 W, the signal output power of 2.57 W is demonstrated at 1551.1 nm with a linewidth of 0.07 nm, corresponding to a slope efficiency of 16.1%. Different from traditional inversion lasers, the narrow-linewidth wavelength tunability of approximately 1.55 μm can be realized by changing the temperature.

Keywords: 1.55 μm ; MgO:PPLN OPO; narrow-linewidth



Citation: Yang, Y.; Lv, G.; Guo, L.; Xu, H.; Kong, H.; Wen, J.; Bian, J.; Ye, Q.; Yang, K.; He, J. 1.55 μm Narrow-Linewidth Pulsed Laser Based on MgO:PPLN. *Photonics* **2023**, *10*, 77. <https://doi.org/10.3390/photonics10010077>

Received: 17 December 2022

Revised: 4 January 2023

Accepted: 8 January 2023

Published: 9 January 2023



Copyright: © 2023 by the authors. Licensee MDPI, Basel, Switzerland. This article is an open access article distributed under the terms and conditions of the Creative Commons Attribution (CC BY) license (<https://creativecommons.org/licenses/by/4.0/>).

1. Introduction

Eye-safe 1.5 μm all-solid-state lasers have the advantages of good beam quality, stable performance, and a compact structure, which has important application value in laser radar, laser rang finding, photoelectric countermeasure, optical communication, etc. [1–3]. In particular, a 1550 nm narrow-linewidth laser is located in the lowest loss transmission window and zero dispersion zone of the zero dispersion shifted fiber, which is widely used in optical fiber communication [4]. At present, a 1.5 μm laser can be obtained based on Er³⁺ doped gain crystals by the energy transition from ⁴I_{13/2} to ⁴I_{15/2}. Considering that single ion doped laser crystals usually emit at 1645 nm or 1615 nm, Yb³⁺ sensitization is usually required [5]. However, the maximum output power of Er³⁺/Yb³⁺ co-doped crystals is only ~2 W due to the low thermal conductivity and the strong up-conversion loss [6]. Another alternative is to utilize nonlinear frequency conversion, such as an optical parametric oscillator (OPO) or a Raman laser [7–10]. The optical parametric oscillator, based on 5 mol% MgO-doped periodically poled lithium niobate (MgO:PPLN) crystals, has attracted extensive attention in recent years due to its high conversion efficiency, wide wavelength tunability and ease of chip integration [11]. However, there is the problem of linewidth broadening caused by high gain for pulsed MgO:PPLN OPOs.

In order to narrow the spectrum, it is an effective method to add frequency selection elements, such as a volume Bragg grating (VBG) or a Fabry–Perot (F–P) etalon, in the resonant cavity. Among them, the VBG is the preferred device for high power narrow-linewidth OPOs because of the strong wavelength stability. In 2015, by using the VBG as a reflective mirror, Peng et al. reported a high-power, narrow-bandwidth mid-infrared MgO:PPLN OPO at 2907.55 nm with an idler bandwidth of 0.68 nm and an average output power of 51.7 W, corresponding to a signal wavelength of 1679.11 nm with a bandwidth of 0.12 nm [12]. However, the reflectivity peak of the VBG can only be tuned slightly via temperature tuning with a slope of 0.014 nm/K. In contrast, the F–P etalon can effectively accommodate both wide tuning and a narrow linewidth, which has been applied to realize

continuous-wave single-frequency MgO:PPLN OPOs [13,14]. However, the linewidth compression becomes difficult for pulsed OPOs due to the strong gain, and there are few reports on narrow-linewidth pulsed OPOs [15,16]. In 2013, Peng et al. demonstrated a narrow-linewidth MgO:PPLN OPO using two etalons in a ring cavity. An average output power of 9.5 W was obtained at 1.655 μm , and the linewidth was compressed from 1 nm to 0.05 nm [16]. Therefore, based on the linewidth compression effect of etalons, a narrow-linewidth pulsed OPO at 1550 nm is expected to be realized. However, the use of dual etalons and ring configuration increases the complexity of the device, which is not conducive to the miniaturization of the device or even chip integration.

In this paper, a narrow-linewidth pulsed MgO:PPLN OPO is demonstrated at 1.55 μm by inserting an etalon into a singly resonant V-shaped cavity. When the incident pump power is 18 W, a maximum average output power of 2.57 W is realized with a center wavelength of 1551.1 nm and a full width at half-maximum (FWHM) of 0.07 nm. In addition, the narrow-linewidth wavelength tunability can also be realized by changing the temperature of the oven.

2. Experimental Setup

Figure 1 shows the experiment setup of the narrow-linewidth MgO:PPLN OPO. Based on the asymmetric TEM₀₀-mode flat-flat cavity with the birefringence compensation, a linearly polarized acousto-optical (AO) Q-switched diode-side-pumped Nd:YAG laser is demonstrated using an AO modulator (I-QS027-584G-U5-ST1, Gooch and Housego) [17]. Both of the Nd:YAG rods have a dimension of $\Phi 5 \text{ mm} \times 130 \text{ mm}$ and a doping concentration of 0.6 at.%. The homemade Nd:YAG pulsed laser is used as the pump source, which delivers an average output power of 30 W with a pulse width of 300 ns at a repetition rate of 10 kHz. A 1/2 wave plate and an optical isolator (ISO) are used to adjust the incident pump power. After the ISO, the other 1/2 wave plate is utilized to rotate the polarization state of the pump light to match the best phase condition ($e \rightarrow e+e$). Through a lens with a focal length of 500 mm, the 1064 nm pump light is focused into the channel of MgO:PPLN crystal with the grating period of 30.5 μm , and the corresponding focusing spot diameter is 450 μm . The PPLN crystal, manufactured by HC Photonics, is doped with 5 mol.% MgO with dimensions of $50 \times 8.6 \times 1 \text{ mm}^3$, which is mounted in an oven with a temperature controlling accuracy of 0.1 $^{\circ}\text{C}$. The oven (OV50D) was also purchased from HC Photonics with a temperature controller (TC-038D), and the maximum temperature can be adjusted to 200 $^{\circ}\text{C}$. Both ends are coated with reflectivity (R) $< 0.5\%$ @ 1064 nm, $R < 1\%$ @ 1430–2128 nm, and $R < 5\%$ @ 2128–4800 nm. M1 is a flat input mirror, which is antireflection (AR) coated at 1.064 μm , 3.4–4.3 μm , and high-reflection (HR) coated at 1.4–1.6 μm . M2 (HR@1.4–1.6 μm , HT@1.064 μm , and 3.4–4.3 μm) is a concave mirror with the curvature radius of 500 mm. M3 is a flat output mirror with a transmission (T) of $\sim 10\%$ around 1.4–1.6 μm . The related parameters are summarized in Table 1. To narrow the linewidth of the signal, a 0.35 mm-thick fused silica F-P solid etalon (R = 68% @ 1550 nm on both sides) is inserted into the single resonant cavity at a small angle.

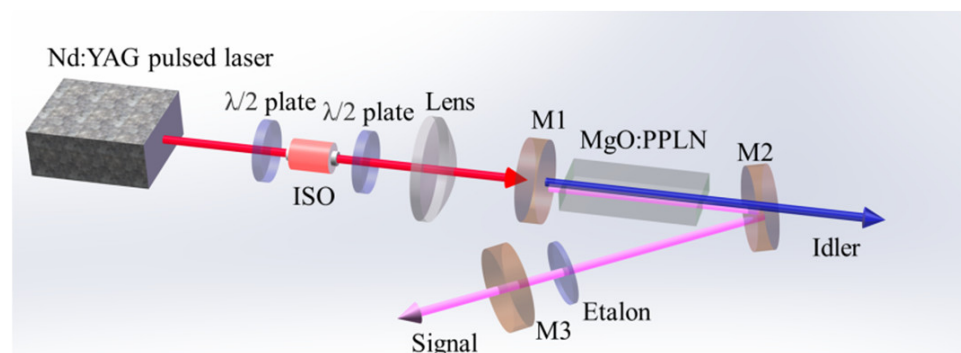


Figure 1. Experiment setup of the narrow-linewidth MgO:PPLN OPO.

Table 1. Mirror parameters used in the OPO and the negative sign represents a concave mirror.

Mirror	Radius	Coating
M1	Infinity	AR@1.064 μm, 3.4–4.3 μm, and HR@1.4–1.6 μm
M2	−500 mm	HR@1.4–1.6 μm, HT@1.064 μm, and 3.4–4.3 μm
M3	Infinity	T = 10%@1.4–1.6 μm

3. Experimental Results

Firstly, the temperature tuning characteristic of the MgO:PPLN crystal is studied without the wavelength-selecting element. In order to achieve the optimal phase matching condition, the polarization state of the pump beam is perpendicular to the optical platform by rotating the 1/2 wave plate. Under an incident pump power of 10 W, the output spectrum of the signal is measured using an AQ6370C spectrum analyzer, which has a resolution of 0.02 nm and a wavelength range of 600–1700 nm. The wavelength at the center of the FWHM is recorded as the center wavelength of the signal wave. As shown in Figure 2, when the temperature of the oven rises from 35 °C to 120 °C at intervals of 5 °C, the signal wavelength increases quasi-linearly from 1546.41 nm to 1579.57 nm with a slope of 0.4 nm/K. The typical spectral width is 0.3 nm, which fluctuates by ±0.05 nm in the temperature range from 35 °C to 120 °C. As shown in the inset of Figure 2, the average output power of the signal is 1.55 W under an incident pump power of 10 W. The power fluctuation is ±4% over the entire temperature range, which indicates that the polarization of the signal is not affected by the crystal temperature. OPO is a second-order nonlinear process involving the interaction of three optical fields, which needs to satisfy the conservation of energy and momentum:

$$\frac{1}{\lambda_p} = \frac{1}{\lambda_s} + \frac{1}{\lambda_i}, \tag{1}$$

$$\frac{n_p}{\lambda_p} - \frac{n_s}{\lambda_s} - \frac{n_i}{\lambda_i} - \frac{1}{\Lambda} = 0. \tag{2}$$

where the parameters λ , n , and Λ represent the wavelength, refractive index, and crystal poling period. The subscripts p , s , and i represent the pump light, signal light, and idler light, respectively. Herein, n is a wavelength and temperature dependent refractive index of e light, and the corresponding Sellmeier equation can be obtained from the reference [18]. A comparison of theoretical and experimental curves is plotted in Figure 2. It is found that the theoretical wavelength is ~5 nm lower than the experimental data, and similar discrepancies can be discovered in the reference [19]. There are two reasons for this phenomenon: one is that the actual temperature of the crystal may be lower than the temperature displayed on the oven because the crystal is exposed to the air, and the other is that the deflection of the crystal angle may lead to a larger actual period. According to the wavelength tuning curve, the temperature of the oven is set to 46 °C to obtain the 1.55 μm signal wavelength. Based on the AO Q-switched Nd:YAG pump source, the OPO output powers versus incident pump powers are shown in Figure 3. With the increase of the incident pump power, the OPO output powers increase almost linearly. Under the incident pump power of 18 W, the maximum signal and idler powers of 4.06 W and 2.04 W are achieved with the slope efficiencies of 23.6% and 12.3%, respectively. As shown in the inset of Figure 3, the center wavelength is 1550.5 nm with a spectral width of approximately 0.5 nm at the maximum pump power.

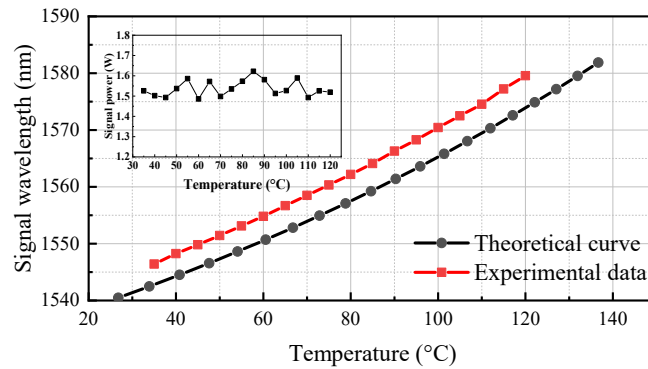


Figure 2. Temperature tuning curves of the signal. Inset: average output power of the signal under an incident pump power of 10 W.

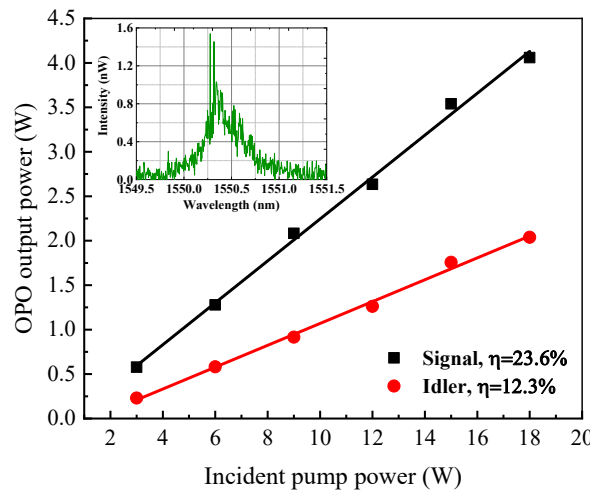


Figure 3. OPO output power versus incident pump power when the temperature is 46 °C. Inset: output spectrum of the signal without the F–P etalon.

Then, inserting the F–P etalon into the cavity, a stable narrow-linewidth OPO output is achieved by optimizing the temperature of the oven. The laser output characteristics are investigated when the MgO:PPLN temperature is set to 46 °C. As shown in Figure 4, the OPO output power linearly increases when the incident pump power exceeds 3 W. Due to the extra loss of the inserted etalon, the output power and efficiency become lower than those without the etalon. Under the incident pump power of 18 W, the maximum output powers of signal and idler waves are 2.57 W and 1.61 W, corresponding to the slope efficiencies of 16.1% and 10.2%. As shown in the inset of Figure 4, the output spectrum of the signal is measured under the maximum pump power. The center wavelength is 1551.1 nm, with a FWHM of 0.07 nm. The corresponding idler wavelength is calculated to be 3388 nm based on Equation (1). At 46 °C, the measured center wavelength fluctuation is approximately ± 0.04 nm within 5 min. The instability of the signal power is approximately $\pm 5\%$ under the influence of the pump power fluctuations. In addition, the narrow-linewidth wavelength tuning can also be realized by changing the crystal temperature. Figure 5 shows the signal spectra at different temperatures, and the corresponding center wavelengths are 1548.63 nm @40 °C, 1550.94 nm @46 °C, and 1553.31 nm @54 °C with a FWHM of approximately 0.05 nm when the incident pump power is approximately 3 W. When the temperature is 46 °C, it can be found that with the increase of the pump power from 3 W to 18 W, the center wavelength of the signal has a red shift of 0.16 nm, which may be caused by the increase of the crystal temperature with the incident pump power. Based on the principle of multi-beam interference, the F–P etalon has different transmission for different

wavelengths. As shown in Figure 5 (dotted line), the corresponding transmittance curve can be plotted using the following transmission formula [20,21]:

$$T(\lambda) = \frac{1}{1 + \frac{4R}{(1-R)^2} \sin^2\left(\frac{4\pi nd \cos \theta}{\lambda}\right)}, \tag{3}$$

where $T(\lambda)$ is the transmission function with respect to the signal wavelength λ , $R = 0.68$ is the reflectivity of the etalon, $n = 1.5$ is the refractive index of the fused silica, $d = 0.35$ mm is the thickness of the F–P etalon, and $\theta = 4.4^\circ$ is the refraction angle of incident beam. The free spectral range (FSR) is given by:

$$FSR = \frac{\lambda^2}{2nd} \text{ (nm)}. \tag{4}$$

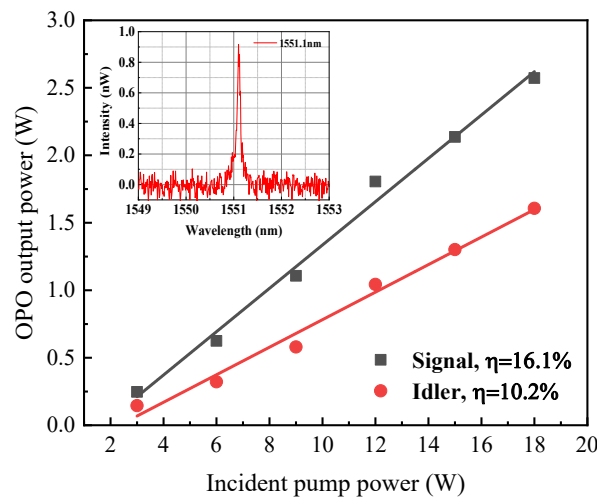


Figure 4. OPO output power versus incident pump power with the F–P etalon. Inset: output spectrum of the signal wave.

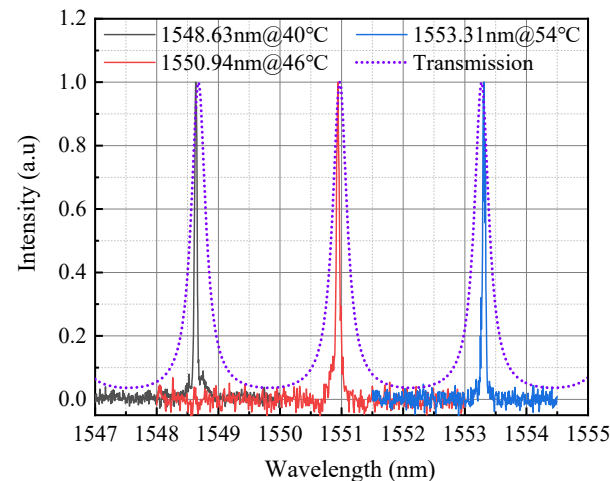


Figure 5. Comparison of the signal spectra (solid lines) and the transmission curve of the etalon (dotted line).

When the signal wavelength λ is 1550 nm, the FSR is theoretically calculated to be approximately 2.29 nm, which is in good agreement with the experimental results. The signal pulse is recorded using a commercial InGaAs photodetector (EOT, ET-3000, USA) and monitored by a digital oscilloscope (InfiniiVision DSOX3014T, KEYSIGHT). The single pulse shape with a pulse duration of 120 ns is shown in Figure 6.

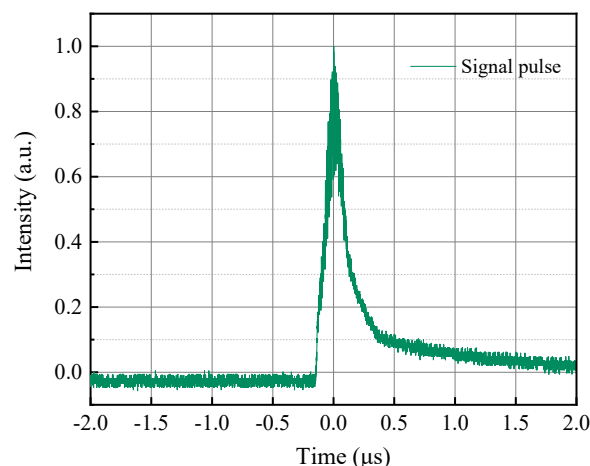


Figure 6. The signal pulse profile with a pulse duration of 120 ns.

4. Conclusions

In conclusion, we have demonstrated a high-power narrow-linewidth $1.55\ \mu\text{m}$ pulsed laser, based on the MgO:PPLN crystal, with a poling period of $30.5\ \mu\text{m}$. Without the wavelength-selecting element, the maximum signal power of $4.06\ \text{W}$ is achieved at $1550.5\ \text{nm}$ with a slope efficiency of 23.6% . To narrow the signal spectrum, a $0.35\ \text{mm}$ -thick F-P etalon is inserted into the single resonant cavity. Under a maximum pump power of $18\ \text{W}$, the signal output power of $2.57\ \text{W}$ is demonstrated at $1551.1\ \text{nm}$ with an FWHM of $0.07\ \text{nm}$, corresponding to a slope efficiency of 16.1% . The idler wavelength is calculated to be $3388\ \text{nm}$ with an average output power of $1.61\ \text{W}$. By changing the crystal temperature, a narrow-linewidth wavelength tuning of approximately $1.55\ \mu\text{m}$ can be realized.

Author Contributions: Y.Y.: investigation, writing-original draft, and funding acquisition. G.L.: investigation. L.G.: writing-review and editing and funding acquisition. H.X., H.K. and J.W.: validation. J.B. and K.Y.: methodology, funding acquisition. Q.Y. and J.H.: conceptualization, software. All authors have read and agreed to the published version of the manuscript.

Funding: This research was funded by the university-level general projects of Anhui University of science and technology (xjyb2020-11); Natural Science Foundation of Anhui Province (2108085QA29); National Natural Science Foundation of China (NSFC) (No. 62105003, No. 62175130); Director Foundation of State Key Laboratory of Pulsed Power Laser Technology (No. SKL2019ZR06, No. SKL2021ZR08); Director Foundation of Advanced Laser Technology Laboratory of Anhui Province (AHL2020ZR03), Scientific Research Foundation for High-level Talents of Anhui University of Science and Technology and High-level Talent Cultivation Funds of State Key Laboratory of Crystal Materials of Shandong University.

Institutional Review Board Statement: Not applicable.

Informed Consent Statement: Not applicable.

Data Availability Statement: Not applicable.

Conflicts of Interest: The authors declare no conflict of interest.

References

1. Päsckke, E.; Leinweber, R.; Lehmann, V. An assessment of the performance of a $1.5\ \mu\text{m}$ Doppler lidar for operational vertical wind profiling based on a 1-year trial. *Atmos. Meas. Tech.* **2015**, *8*, 2251–2266. [[CrossRef](#)]
2. Qi, Y.; Bai, Z.X.; Wang, Y.L.; Zhang, X.P.; Qi, Y.Y.; Ding, J.; Bai, Z.A.; Lu, Z.W. Research progress of all-solid-state passively Q-switched Er:Yb:glass lasers. *Infrared Phys. Techn.* **2021**, *116*, 103727. [[CrossRef](#)]
3. Kasmi, M.; Mrabet, H.; Mhatli, S.; Bahloul, F.; Dayoub, I.; Oh, K. Performance enhancement of $64\ \text{Gb/s}$ OFDM system at $1550\ \text{nm}$ over multimode fiber using Volterra equalization. *Opt. Commun.* **2019**, *449*, 86–93. [[CrossRef](#)]
4. Aliee, M.; Mozaffari, M.H.; Saghaei, H. Dispersion-flattened photonic quasicrystal optofluidic fiber for telecom C band operation. *Photonic. Nanostruct.* **2020**, *40*, 100797. [[CrossRef](#)]

5. Guo, L.; Li, M.; Li, T.; Zhang, S.Y.; Yang, K.J.; Fan, M.Q.; Zhao, S.Z. Inband pumped passively Q-switched Er: YAG laser at 1645 nm using WS₂. *Opt. Commun.* **2018**, *406*, 230–233. [[CrossRef](#)]
6. Chen, Y.H.; Huang, J.H.; Huang, Y.D.; Gong, X.H.; Lin, Y.F.; Luo, Z.D.; Chen, Y.J. Refractive index, thermal, spectroscopic and 1.55 μm laser properties of an Er: Yb: Lu₂Si₂O₇ crystal. *Opt. Mater.* **2022**, *128*, 112448. [[CrossRef](#)]
7. Peng, Y.F.; Wei, X.B.; Wang, W.M.; Li, D.M. High-power 3.8 μm tunable optical parametric oscillator based on PPMgO:CLN. *Opt. Commun.* **2010**, *283*, 4032–4035. [[CrossRef](#)]
8. Peng, Y.F.; Wei, X.B.; Luo, X.W.; Nie, Z.; Peng, J.; Wang, Y.; Shen, D.Y. High-power and widely tunable mid-infrared optical parametric amplification based on PPMgLN. *Opt. Lett.* **2016**, *41*, 49–51. [[CrossRef](#)]
9. Zhang, H.N.; Chen, X.H.; Wang, Q.P.; Zhang, X.Y.; Chang, J.; Gao, L.; Shen, H.B.; Cong, Z.H.; Liu, Z.J.; Tao, X.T.; et al. High-efficiency diode-pumped actively Q-switched ceramic Nd:YAG/BaWO₄ Raman laser operating at 1666 nm. *Opt. Lett.* **2014**, *39*, 2649–2651. [[CrossRef](#)]
10. Ma, H.J.; Wei, X.; Dai, S.B.; Yin, H.; Zhu, S.Q.; Li, Z.; Chen, Z.Q. Intra-cavity diamond Raman laser at 1634 nm. *Opt. Express.* **2021**, *29*, 31156–31163.
11. Jin, H.; Liu, F.M.; Xu, P.; Xia, J.L.; Zhong, M.L.; Yuan, Y.; Zhou, J.W.; Gong, Y.X.; Wang, W.; Zhu, S.N. On-chip generation and manipulation of entangled photons based on reconfigurable lithium-niobate waveguide circuits. *Phys.Rev.Lett.* **2014**, *113*, 103601. [[CrossRef](#)] [[PubMed](#)]
12. Peng, Y.F.; Wei, X.B.; Nie, Z.; Luo, X.W.; Peng, J.; Wang, Y.; Shen, D.Y. High-power, narrow-bandwidth mid-infrared PPMgLN optical parametric oscillator with a volume Bragg grating. *Opt. Express.* **2015**, *23*, 30827–30832. [[CrossRef](#)] [[PubMed](#)]
13. Li, K.; Yang, S.H.; Wang, X.; Li, Z.; Zhang, J.Y. Frequency Chirped Intensity Modulated Mid-Infrared Light Source Based on Optical Parametric Oscillation. *IEEE Photonics J.* **2020**, *12*, 1–9. [[CrossRef](#)]
14. Zhao, J.Q.; Cheng, P.; Xu, F.; Zhou, X.F.; Tang, J.; Liu, Y.; Wang, G.D. Watt-level continuous-wave single-frequency mid-infrared optical parametric oscillator based on MgO:PPLN at 3.68 μm. *Appl. Sci.* **2018**, *8*, 1345. [[CrossRef](#)]
15. Xing, T.L.; Wang, L.; Hu, S.W.; Cheng, T.Q.; Wu, X.Y.; Jiang, H.H. Widely tunable and narrow-bandwidth pulsed mid-IR PPMgLN-OPO by self-seeding dual etalon-coupled cavities. *Opt. Express.* **2017**, *25*, 31810–31815. [[CrossRef](#)]
16. Peng, Y.F.; Wei, X.B.; Xie, G.; Gao, J.R.; Li, D.M.; Wang, W.M. A high-power narrow-linewidth optical parametric oscillator based on PPMgLN. *Laser Phys.* **2013**, *23*, 055405. [[CrossRef](#)]
17. Guo, L.; Yang, Y.Y.; Xu, H.P.; Kong, H.; Lv, G.R.; Wen, J.Q.; Bian, J.T.; Ye, Q.; Sun, X.Q.; Yang, K.J. High power linearly polarized diode-side-pumped Nd: YAG laser based on an asymmetric flat–flat resonator with the variable working point. *Opt. Commun.* **2022**, *520*, 128453. [[CrossRef](#)]
18. Gayer, O.; Sacks, Z.; Galun, E.; Arie, A. Temperature and wavelength dependent refractive index equations for MgO-doped congruent and stoichiometric LiNbO₃. *Appl. Phys. B.* **2008**, *91*, 343–348. [[CrossRef](#)]
19. Xu, L.; Zhang, S.Y.; Chen, W.B. Tm:YLF laser-pumped periodically poled MgO-doped congruent LiNbO₃ crystal optical parametric oscillators. *Opt. Lett.* **2012**, *37*, 743–745. [[CrossRef](#)]
20. Liu, J.L.; Chen, X.Y.; Wang, R.M.; Wu, C.T.; Jin, G.Y. A stable wavelength operation Ho:YAG laser with orthogonally polarized pump. *Chinese Phys. Lett.* **2019**, *36*, 024201. [[CrossRef](#)]
21. Ahmad, H.; Muhamad, A.; Sharbirin, A.S.; Samion, M.Z.; Ismail, M.F. Tunable Q-switched thulium-doped Fiber Laser using multiwall carbon nanotube and Fabry-Perot Etalon filter. *Opt. Commun.* **2017**, *383*, 359–365. [[CrossRef](#)]

Disclaimer/Publisher’s Note: The statements, opinions and data contained in all publications are solely those of the individual author(s) and contributor(s) and not of MDPI and/or the editor(s). MDPI and/or the editor(s) disclaim responsibility for any injury to people or property resulting from any ideas, methods, instructions or products referred to in the content.